IMPLEMENTATION OF DIFFERENT CURRENT-CONTROLLED PWM STRATEGIES FOR VSI

‡Hossein M. Kojabadi, *Idris A. Gadoura and §Mohsen Ghribi

‡*Sahand University of Technology, Tabriz, Iran*
**University of New Brunswick, Fredericton, Canada*
§*Université de Moncton, Moncton, Canada*
(hmadadi64@yahoo.ca, igadoura@unb.ca, ghribim@umoncton.ca)

Abstract: Many current-controlled PWM methods have been proposed to design high performance of current control for grid-connected inverters in distributed power generation systems. However none of them have good performance in providing low THD and, at the same time, good robustness to parameters mismatch. Two different current control methods, namely, traditional predictive current controller and robust predictive current controller are discussed in this paper. First technique is based on the generalization of existing methods. Although these two schemes can provide good power quality for distributed power generation systems, the proposed technique is superior to another one in achieving more precise current control with minimum distortion and harmonic noise, and at the same time, less sensitive to filter parameter mismatch.

Keywords: Inverters, PWM, Prediction methods, robust control.

1. INTRODUCTION

In recent years, distributed power generation (DG) systems have shown a tremendous market potential. Usually grid-connected voltage-source inverters (VSI) are employed to interface the DG systems with power grids. In order to feed grids with high quality power, the current control of the grid-connected VSI plays an important role since the DG system will not regulate the voltage at the point of common coupling to meet the requirements of the IEEE standards and then the power quality mainly depends on the output current (IEEE Standards, 2003). For an inverter-based distributed power generator, the power quality largely depends on the performance of inverter controller (Takahshi, 1982). Pulse Width Modulation (PWM) is the most popular control technique in voltage-source inverters. As compared to the open loop voltage PWM converters, the current-controlled PWM has several advantages (Kazmierkowski, 1998). Most applications of voltage-source PWM converters such as: AC power supply systems, AC motor drives and UPS systems have a current feedback loop as a part of their control structure. Current controllers can be classified as hysteresis, ramp comparison or predictive controllers (Schonung and Stemmler, 1964). Hysteresis current controllers, presented in (Plunkett, 1979), utilize hysteresis in comparison of load currents to current references. Hysteresis current controllers have the advantage of simplicity and robustness, but converter's switching frequency largely depends on the load parameters and, consequently, the load current harmonics ripple is not optimum. Improved hysteresis control strategies were proposed in (Bose, 1990) and (Yao and Holmes, 1993), which presented the variable-hysteresis-band current control technique. This control method, where the band is modulated with the system parameters, maintains a nearly constant switching frequency, however the current ripple is still not optimum. (Pan, *et al.*, 2003) proposed the switch status dependent inner bound current control strategy where an adaptive inner bound is modulated to reduce switching frequency while guaranteeing current error in a specified bound. Predictive controllers calculate the inverter voltages required to force the currents to follow the current reference see (Holtz and Stadtfeld, 1983) and (Holmes and Martin, 1996). This method offers the potential for achieving more precise current control with minimum distortion and harmonic noise, however, takes more calculations and requires a good knowledge of the system parameters. The implementation of predictive strategies into digital controllers has been of particular interest in recent studies. In (Holtz and Stadtfeld, 1983) and (Holmes and Martin, 1996), the digital predictive current

controllers for single-phase and three-phase voltage-source inverters are proposed. This method fully compensates for the computational delays and sampling delays errors but the controller has a poor robustness in real system. The predictive controllers need good knowledge of the system parameters. If there are model mismatch in the control system, the mismatch will influence the control accuracy.

In this paper the robust predictive current controller for grid-connected single-phase inverters is proposed. Simulation and experimental results demonstrate the superiority of the proposed method over existing methods. The experimental tests will show that the inverter with the proposed predictive current controller has better robustness than the inverter with the traditional predictive current controller. Later, the model mismatch influence on two predictive controllers will be discussed.

2. ROBUST PREDICTIVE CURRENT-CONTROLLED PWM STRATEGY

2.1 Signal-phase full-bridge VSI

The single-phase full bridge voltage source inverter topology is shown in Fig.1. It is composed of a dc voltage source, four power switches and a filter inductor.

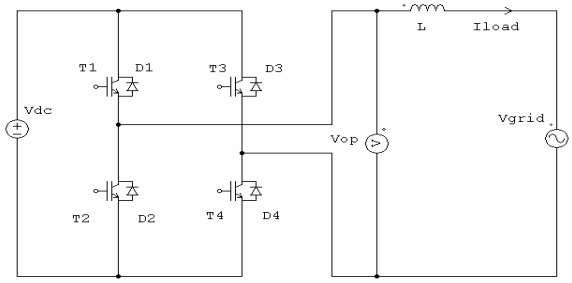

Fig.1 Single-phase grid-connected full bridge voltage source inverter

The full-bridge inverter's operation can be divided into four modes; two modes in positive load current period, and two modes in negative load current period, as described in Table 1.

Table 1 Inverter operational modes

M	$\mathbf{T_1}$	$\mathbf{T_2}$	$\mathbf{T_3}$	$\mathbf{T_4}$	$\mathbf{D_3}$	$\mathbf{D_4}$	$\boldsymbol{V_{op}}$	$\boldsymbol{I_{load}}$
1	on	off	off	on	off	off	V_{dc}	pos
2	on	off	off	off	on	off	0	pos
3	off	on	on	off	off	off	$-V_{dc}$	neg
4	off	on	off	off	off	on	0	neg

2.2 Current controller strategies for VSI

For inverter based DG systems, the inverters are connected to the existing grid, so that the output voltage cannot be controlled. The power quality is defined by the output current quality. Pulse width modulation is the most popular control technique in voltage-source inverters. As compared to the open loop voltage PWM converters, the current-controlled PWM has several advantages. One of the advantages is to control the current injected into grid with low distortion and harmonic noise. The strategies of current controllers can be classified as ramp comparison controllers, hysteresis controllers, and predictive controllers. The ramp comparison controller compares the current errors to triangle wave to generate the inverter firing signals. The hysteresis controllers utilize some type of hysteresis in the comparison of the currents to the current reference. The predictive controllers calculate the inverter voltages required to force the currents to follow the current reference.

2.3 Traditional predictive current controller

(Holmes and Martin, 1996) proposed an algorithm for directly implementing a predictive current controller in a microprocessor for load condition where the load voltage is known. The proposed method, in (Holmes and Martin, 1996), compensates for errors caused by digital sampling and computing delays. The algorithm uses the results of previous switching cycles to forward estimate both the future grid voltage and future load current. From Fig. 1 it is clear that the inverter load current (i_{load}) is decided by following differential equation:

$$V_{op} = V_{grid} + L\frac{di_{load}}{dt} \qquad (1)$$

where V_{grid} is the grid voltage, V_{op} is the output voltage, i_{load} is the output current, and L is the filter's inductance in mH.

Assuming that the inverter is operating with a constant switching frequency, the switching period will be a constant value, T_{period}. In the switching period [n, n+1], equation (1) can be written in a discrete form, as:

$$V_{op\_av}[n] = V_{grid\_av}[n] + L\frac{I_{load}[n+1] - I_{load}[n]}{T_{period}} \qquad (2)$$

where $V_{op\_av}[n]$, $V_{grid\_av}[n]$ are the average inverter output voltage and average grid voltage over the switching period [n,n+1], respectively, and $I_{load}[n+1]$, $I_{load}[n]$ are the measured load currents at the sampling point [n+1] and [n], respectively. The timing schematic is shown in Fig. 2.

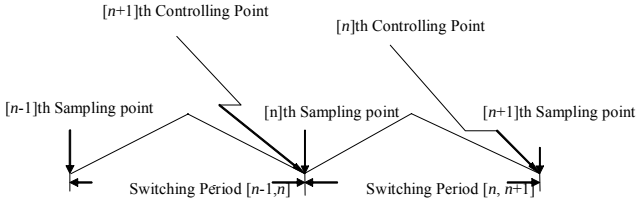

Fig. 2. Timing schematic of switching periods and sampling points

The target of the controller is making the load current at the sampling point [n+1], I_{load} [n+1] equal to the

reference current value at the end of the switching period [n, n+1], $I_{ref}[n+1]$. Consequently the predictive average output voltage $V_{op\_av}[n]$ turns to be:

$$V_{op\_av}[n] = V_{grid\_av}[n] + L\frac{I_{ref}[n+1] - I_{load}[n]}{T_{period}} \quad (3)$$

The practical implementation will require computational time to solve for the $V_{op\_av}[n]$. As illustrated in Fig. 2, traditional predictive algorithm does the computation in the previous switching period [n-1, n]. This means that the measured values of current, I_{load} [n-1], and grid voltage, V_{grid} [n-1], are only available up to time [n-1] before the calculation proceed. The controller will predict the I_{load} [n]and V_{grid} [n] and calculate the demand inverter output voltage $V_{op\_av}[n]$. And then in this way, controller controls the four switches at controlling point of [n-1]. To predict, $V_{grid\_av}[n]$, the average grid voltage over switching period [n, n+1], assume that the change of grid voltage over the switching period is linear and the grid voltage change over the switching period [n, n+1] is equal to the change of the switching period [n-1, n]. Then, $V_{grid\_av}[n]$ can be estimated from previously measured voltages using a simple linear extrapolation:

$$V_{grid\_av}[n] = \frac{5}{2}V_{grid}[n-1] - \frac{3}{2}V_{grid}[n-2] \quad (4)$$

I_{load} [n] can be estimated by adding the predicted current change during the switching period [n-1, n] to the measured current at time[n-1].

$$I_{load}[n] = I_{load}[n-1] + \frac{T_{period}}{L}\left(V_{op\_av}[n-1] - \frac{3V_{grid}[n-1] - V_{grid}[n-2]}{2}\right) \quad (5)$$

By substituting (4) and (5) into (3) the demand average output voltage applied in the switching period [n, n+1], is:

$$V_{op\_av}[n] = 4V_{grid}[n-1] - 2V_{grid}[n-2] - V_{op\_av}[n-1] + L\frac{I_{ref}[n+1] - I_{load}[n-1]}{T_{period}} \quad (6)$$

2.4. Robust predictive current controller

Laboratory tests show that the traditional predictive current algorithm has poor robustness to model parameters mismatch, such as filter's inductance. The error between the actual and model filter inductance will cause the inverter output current to oscillate. A robust predictive current controller with better robustness to parameters mismatch is proposed. As mentioned before, the predictive average output voltage $V_{op\_av}[n]$ is:

$$V_{op\_av}[n] = V_{grid\_av}[n] + L\frac{I_{ref}[n+1] - I_{load}[n]}{T_{period}}$$

The traditional predictive algorithm does the computation in the previous switching period to compensate the error introduced by sampling and computation delays. In experiment, the delays can be measured. For TMS320-2407A the delays is around 10 μs. Fig. 3 illustrates the delays as TD (Total Delay). Compared to 16.6 ms cycle period of 60 Hz grid voltage and current frequency, 10μs is negligible that one can assume the sampled grid voltage and load current are unchanged in this period.

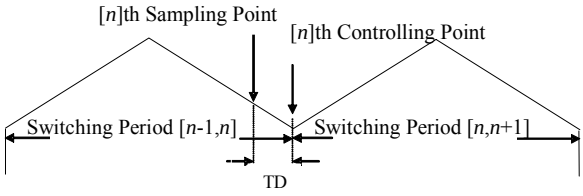

Fig. 3 Timing schematic of sampling point and controlling point

As illustrated in the Fig. 3, the sampling point is set just ahead of controlling point by the period of the TD. With the above assumption, the measured values of current, I_{load} [n], and grid voltage, V_{grid} [n], are available up to instant [n] before the calculation proceed to predict the demanded output voltage of inverter. To predict, V_{grid_av} [n], the average grid voltage over switching period [n, n+1], assume that the change of grid voltage over the switching period is linear and the grid voltage change over the switching period [n, n+1] is equal to the change of the switching period [n-1,n]. Then, V_{grid_av} [n] can be obtained from the measured grid voltage, V_{grid} [n], V_{grid_av} [n-1], as:

$$V_{grid\_av}[n] = 1.5\,V_{grid}[n] - 0.5\,V_{grid}[n-1] \quad (7)$$

Substituting the (7) and (5) into (3), the predictive average output voltage of the inverter over the switching period [n,n+1]:

$$V_{op\_av}[n] = (1.5 + \frac{L_m}{T_{period}L})V_{grid}[n] - 0.5\,V_{grid}[n-1] - \frac{L_m}{L}V_{op\_av}[n-1] + \frac{L}{T_{period}}I_{ref}[n+1] - \frac{L_m}{T_{period}}I_{load}[n-1] \quad (8)$$

3. SIMULATION RESULTS

Two current controlled PWM strategies: traditional predictive current controller and robust predictive current controller are verified by the simulation using PSIM software package. For all simulations, the dc voltage is 400 V, grid voltage is 240 V, filter inductor is 2 mH, and output power is 10 kW. The simulation results of traditional current predictive controller is shown in Fig. 4. The switching frequency of IGBTs sets at 10 kHz. The current THD is 2.8% at 10 kW. The simulation results of robust current predictive controller is shown in Fig. 5. The switching frequency of IGBTs sets at 10 kHz. The current THD is 2.6% at

10 kW. Both predictive control algorithms meet the IEEE Standard 1547 requirement of THD, which is below 5% (IEEE Standard, 2003). The predictive controllers need good knowledge of the system parameters. If there are model mismatch in the control system, the mismatch will influence the control accuracy (Yu, 2004).

4. EXPERIMENTAL RESULTS

The proposed predictive current control strategy is tested on a 10 kW prototype grid-connected single-phase IGBT inverter, as shown in Fig. 1. The prototype IGBT inverter includes a power circuit module, an interfacing and sensing module, a DSP-based control module, and an IGBT driver module (Yu, 2004). The input of the inverter is connected to a three-phase generator driven by wind turbine or micro gas-turbine. The rated input line-line voltage from the generator is 280 V, corresponding to a dc link voltage of 390 V. The output of the inverter is connected to the grid. The normal grid voltage is 240 V and grid frequency is 60 Hz. The rated output current is 42 A. The inverter is equipped with software and hardware protections including over-current of dc link and inverter output, over-temperature of IGBT, over-voltage of the grid, dc link and generator, under-voltage of the grid and generator, over-frequency of the grid, under-frequency of the grid voltage. Inverter output current and grid voltage for the proposed method is shown in Fig. 6. Total harmonics distortion of grid voltage is 2.3% and total harmonics distortion of inverter output current is 0.9% measured by power quality analyzer. This THD is much smaller than that proposed by IEEE standards of 5%. Predictive output voltage is calculated based on (8).

5. STABILITY ANALYSIS

In order to investigate the proposed method's robustness to the mismatch of filter parameter, L, the robustness issues of two predictive methods will be compared.

5.1 Influence of model mismatch on the system stability

From equations (5), (6), and (8), the characteristic equations of two systems can be derived, it is worth noting that both systems are second-order system. The relative error between the actual and modeled inductance, ΔL, will influence the location of closed-loop poles. This model mismatch will influence the transient response characteristics and the stability of the two systems. The relative error of inductance, ΔL, could be positive or negative. The positive relative error implies that the modeled inductance value is smaller than actual inductance value. The negative relative error implies that the modeled inductance value is bigger than actual inductance value. For traditional predictive current controller, the poles of closed-loop systems in z-plane are $p_{1,2} = \pm\sqrt{\Delta L}$. When relative inductance error is positive, one pole is on positive half real axis and another one is on negative half real axis. When relative inductance error is negative, one pole is on positive half imaginary axis and another one is on negative half imaginary axis. On the other hand, for robust predictive current controller, the poles of closed-loop systems in z-plane are $p_1 = 0$ and $p_2 = \Delta L$. When relative inductance error is positive, one pole is on positive half real axis and another one is at origin. When relative inductance error is negative, one pole is on negative half real axis and another one is at the origin.

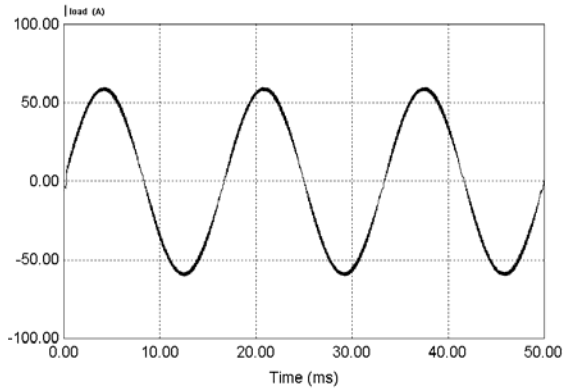

Fig. 4 Output current waveform of inverter with traditional predictive controller

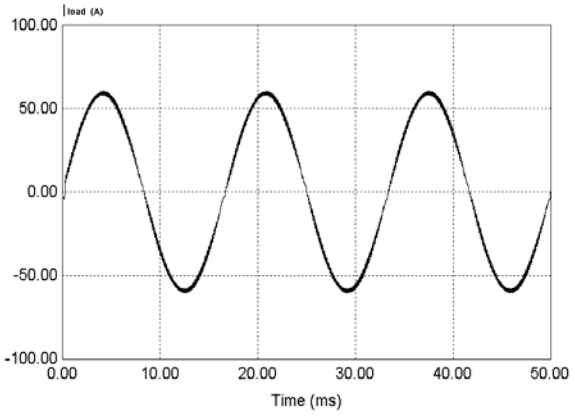

Fig. 5 Output current waveform of inverter with robust predictive controller

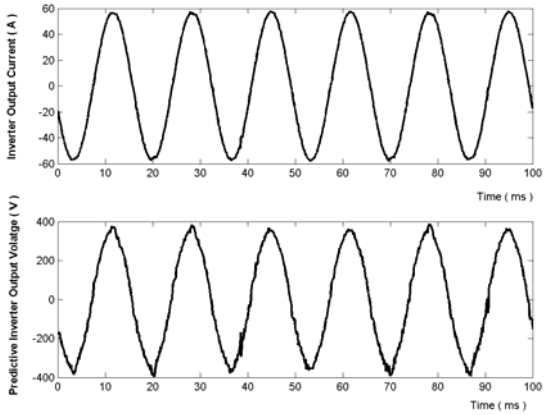

Fig. 6 Output current and output voltage waveforms for proposed method

Fig. 7 illustrates the closed-loop poles of traditional and robust system. From Fig. 7 it is worth noting that with $L_m \geq 2L$ the poles will be on or outside the unit

circle and, therefore, both systems will be unstable as shown in Fig. 8 and Fig. 9. First, the stable range of two systems is discussed with respect to the relative error between the actual and modeled inductance. The stable criterion of controlled system in *z*-plane is that the poles of closed-loop system are located inside the unit circle. For both systems, the stable range of relative error of inductance is

$-1 \leq \Delta L \leq 1$ and $\Delta L = 1\text{-}L_m/L$

Therefore, the stable range of modeled filter inductance for traditional and robust predictive systems is:

$0 \geq L_m \geq 2L$

Thus, both systems have the same stable range of modeled filter inductance.

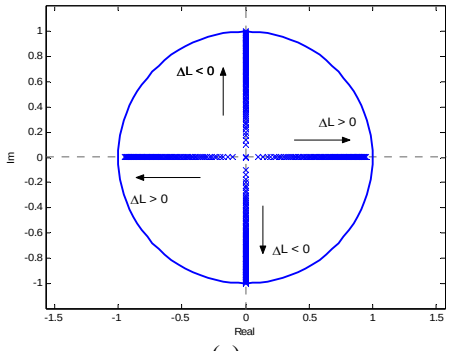

(a)

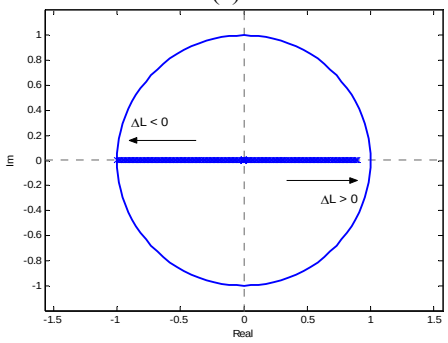

(b)

Fig. 7 The closed-loop poles with changing of ΔL for traditional (a), and robust systems (b)

5.2 Comparison of two predictive algorithms by experimental tests

To confirm the conclusion in Section 5.1, the modeled filter inductance, L_m, is set to four different values (L_m =L, 1.3*L, 1.6*L, 2.0*L) in the experiments to see the model mismatch influence on two systems. The tests have been done on a 10 kW prototype inverter with 2 mH filter inductor. The digital controller implements two predictive algorithms separately. The output power of inverter is set at 3 kW; and dc link voltage was 380 V. The predictive average output voltage, V_{op_av}, and inverter output current are monitored in order to compare. Fig. 8 illustrates experimental results of system whose controller implements the traditional predictive algorithm, where modeled inductance is bigger than actual inductance. The one can note that predictive output voltage and load current begin to oscillate when ΔL = -30%. The oscillation turns to more obviously when ΔL = -60%. When ΔL = -100%, the predictive output voltage and load current oscillate continuously. This confirms the analysis in previous Sections 5.1 that traditional system turns instable when model inductance is two times bigger than actual inductance. Fig. 9 illustrates experimental results of proposed system whose controller implements the robust predictive algorithm, where modeled inductance is bigger than actual inductance. The one can note that predictive output voltage and load current begin to oscillate when ΔL = -60%. When ΔL = -100%, the predictive output voltage and load current oscillate continuously. Also the proposed system turns instable when model inductance is two times bigger than actual inductance. By comparing both Fig. 8 and Fig. 9, it is worth noting that both systems start to oscillate continuously when modeling inductance is two times bigger than actual one, but the magnitude of perturbations in the traditional method is much bigger than the proposed one. In addition, for $|\Delta L| \leq 100\%$, the proposed method has acceptable output current waveform with small THD. However, the traditional method has unacceptable THD for $|\Delta L| \leq 30\%$.

6. CONCLUSION

Simulation and experimental results confirm that the predictive current controllers in grid connected inverters provide acceptable THD value based on IEEE standards. The theoretical analysis and experiment results proved that model mismatch of filter inductor influences the system stability and transient response characteristics. For predictive controller, accuracy of the model will affect the controller's performance dramatically. Comparing two predictive control algorithms, the system that implements the proposed algorithm is more robust than the system implements the traditional predictive algorithm.

REFERENCES

Bose, Bimal K. (1990). " An Adaptive Hysteresis-Band Current Control Technique of a Voltage-fed PWM Inverter For Machine Drive System," *IEEE Trans. on Industrial Electronics,* Vol. 37, pp. 402-408.

Holmes, D. G., and D. A. Martin (1996) "Implementation Of A Direct Digital Predictive Current Controller For Single And Three Phase Voltage Source Inverter," *Proc. of the 1996 IEEE Conf. on Industry Applications*, pp. 906-913.

Holtz, J., and S. Stadtfeld (1983). "A Predictive Controller For The Stator Current Vector Of AC Machines Fed From A Switched Voltage Source," *Proc. of the 1983 IEEE Conf. on Power Electronics*, pp 1665-1675.

IEEE Standard (2003). IEEE Standard 1547, *Standard for Interconnecting Distributed Resources with Electric power systems.*

Kazmierkowski, M. P. (1998). "Current Control Techniques For Three-Phase Voltage-Source PWM Converters: A Survey," *IEEE Trans. on Industrial Electronics*, Vol. 45, pp. 691-701.

Pan, Ching-Tsai, Yi-Shuo Huang and Tai-Lang Jong (2003). "A constantly sampled current controller with switch status dependent inner bound," *IEEE Trans. on Industrial Electronics* , Vol. 50, pp.528 – 535.

Plunkett, B. (1979). "A current controlled PWM transistor inverted drive," *Proc. of the 1979 IEEE Conf. IAS Annual Meeting*, pp. 785-792.

Schonung, A., and H. Stemmler (1964). " Static Frequency Changers With 'Subharmonic' Control In Conjuction With Reversible-Speed Ac Drives," Brown Boveri Rev., pp. 555-577.

Takahshi, I., (1982). "A flywheel energy storage system having harmonics power compensation," University of Wisconsin, Madison ,WEMPEC Res., Rep.82-3.

Yao, Qunying and D. G. Holmes (1993). "A Simple, Novel Method For Variable-Hysteresis-Band Current Control of A Three Phase Inverter With Constant Switching Frequency," *Proc. of the 1993 IEEE Industry Applications Meeting*, pp.1122-1129.

Yu, Bin (2004). "Predictive Current-controlled PWM Strategy for Grid-connected Single-phase Inverter," University of New Brunswick, MSC Thesis.

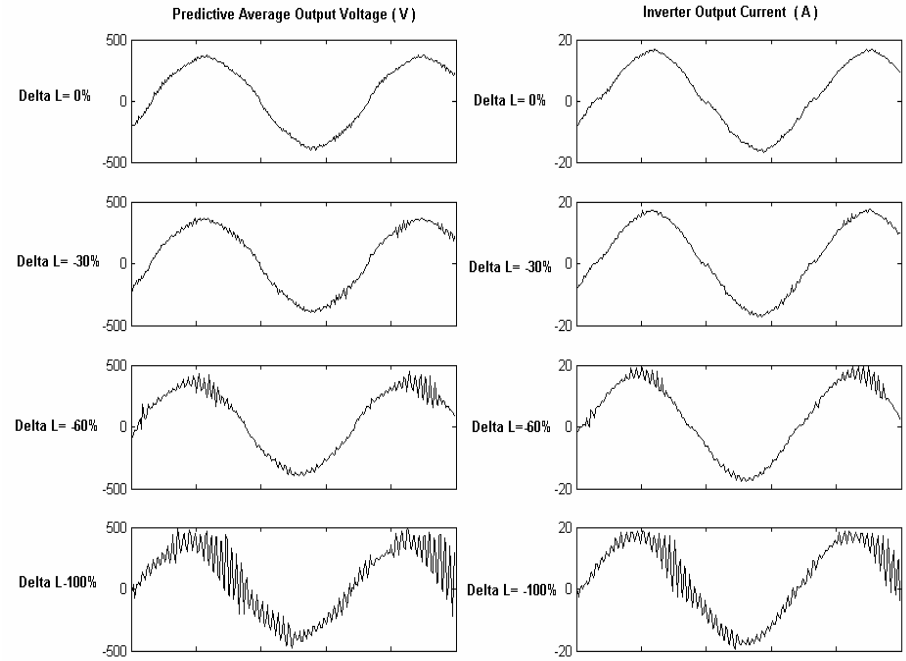

Fig. 8 Model mismatch influence on traditional method, (ΔL<0)

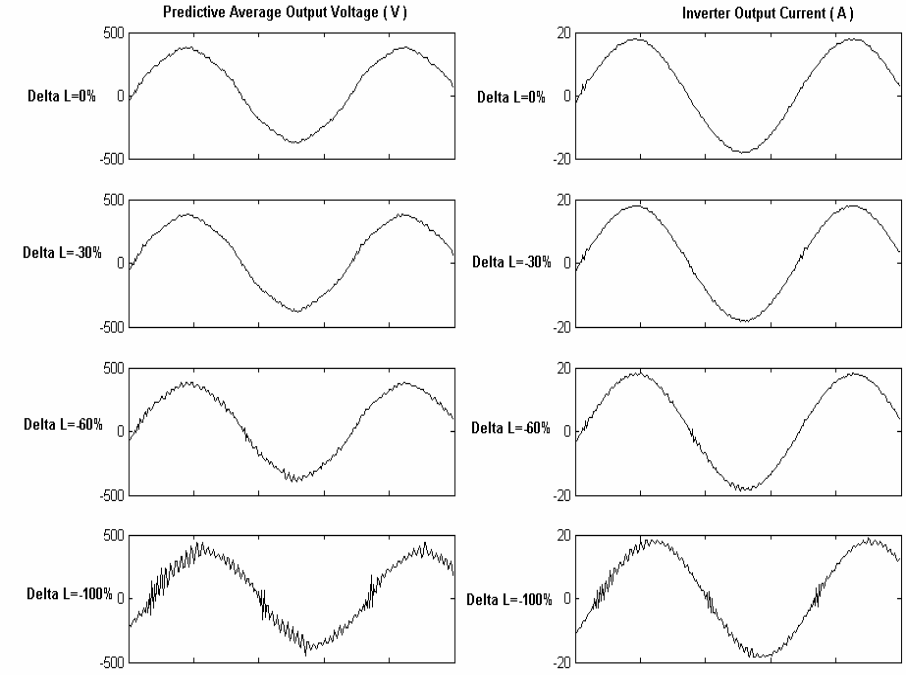

Fig. 9 Model mismatch influence on proposed method, (ΔL <0)